



# An evaluation of the minor isotope ratio uncertainties based on traceable standards from new brunswick laboratory

Kattathu J. Mathew<sup>1</sup> · Chelsea Ottenfeld<sup>1</sup> · Nicholas Butterfield<sup>1</sup>

Received: 12 April 2022 / Accepted: 17 August 2022 / Published online: 10 September 2022  
© Akadémiai Kiadó, Budapest, Hungary 2022

## Abstract

Certified reference material (CRM) standards are used for calibration of mass spectrometer instruments, for measurement control, and for validating analytical methods used by safeguards laboratories. We evaluated the minor isotopic data on plutonium CRMs 136, 137, 138, and 126-A to estimate the contributing factors to the uncertainty budgets of these ratios. Data evaluated were obtained using the total evaporation methodology, which is considered the gold standard for major ratio measurements. For the minor isotope ratios, the per turret correction yielded overall uncertainties that are a factor of 2 to 3 smaller than the correction based on an assumed correction factor using the specified abundance sensitivity. LA-UR-22–22,150.

**Keywords** Thermal ionization mass spectrometry · Isotope ratios · Plutonium · Total evaporation · Correlation effects · Nuclear forensics

## Introduction

Thermal ionization mass spectrometry (TIMS) is considered the gold-standard in isotope ratio measurements for chronometry in geochemistry and cosmochemistry and for safeguards measurements as well as nuclear forensics. Total evaporation (TE) method [1–6] using TIMS instrumentation has proven to be very useful in reducing the measurement uncertainty of the major ratio measurements of actinide elements. The improvement in the uncertainty of the isotope ratio measurements using TE has been utilized in the recent certification of uranium standards [7–13] and to a limited extent in latest certification of plutonium standards.

For minor isotope ratio measurements, the TE methodology yields ratios that are systematically biased due to tailing of the major isotope signals into the lower mass isotope signals [2, 6]. The tailing correction is mostly dependent of the vacuum level in the instrument as it is caused by ions losing energy in collisions with neutral species during their acceleration in the high voltage electric field, separation of the different isotopes in the magnetic field, and flight to the detectors aligned to collect the different isotopic signals.

Factors like the width of the sample load are also perceived to have an influence on the distribution of the energy of the isotopic beam in the instrument.

The abundance sensitivity characteristics vary between TIMS instruments from different manufacturers, as the actual operating voltages, the geometry and design of the source and detector housing, and the efficiency of the vacuum systems are different. For Faraday isotope ratio measurements using TIMS instrumentation, two different methodologies for correcting the minor isotope ratios for systematic biases originating from tailing have been adopted: i) based on manufacturer specified or measured abundance sensitivity characteristics of the instrument, and ii) through quantification of the systematic biases using standards certified for the minor isotope ratios and correcting the samples/standards analyzed together as a suite. Measurement of the  $^{244}\text{Pu}/^{239}\text{Pu}$  isotope ratio, at trace levels, often involves the use of an ion counter (for example, Secondary Electron Multiplier – SEM) and are not considered here as other unique uncertainty components are applicable to these measurements. In this paper, we compare the uncertainties realized by these two correction methodologies for  $^{238}\text{Pu}/^{239}\text{Pu}$ ,  $^{241}\text{Pu}/^{239}\text{Pu}$ , and  $^{242}\text{Pu}/^{239}\text{Pu}$  minor isotope ratios using TE methodology and recommend the data evaluation technique that is more reliable for eliminating this systematic bias in these minor isotope ratios.

✉ Kattathu J. Mathew  
kmathew@lanl.gov

<sup>1</sup> Actinide Analytical Chemistry, Los Alamos National Laboratory, Los Alamos, NM 87544, USA

## Experimental

All data presented here were obtained using the Triton (manufacturer: Thermo Scientific, Bremen, Germany) multi-collector TIMS instrument. The TE analytical methodology with the cup configuration shown in Table 1 was used for the data collection. Double filament configuration using zone refined rhenium (both sample filament and ionization filament are made from pre-fabricated rhenium) was used for analysis. Samples/standards were analyzed in an auto sequence following daily calibrations that included baseline, gain, focus on  $^{187}\text{Re}$ , and peak centering on masses  $^{185}\text{Re}$ ,  $^{187}\text{Re}$ ,  $^{239}\text{Pu}$ , and  $^{240}\text{Pu}$ . Pre-analysis steps for each sample/standard included focus and peak centering on  $^{187}\text{Re}$  and  $^{240}\text{Pu}$  (masses in the center cup). 1-s integration time was used for TE data acquisition.

TE analysis used a sum ( $^{239}\text{Pu} + ^{240}\text{Pu} + ^{241}\text{Pu} + ^{242}\text{Pu}$ ) target intensity of 6 V. The tailing corrections were performed using two methodologies: (i) using an abundance sensitivity correction from the instrument manufacturer and ii) evaluation of the magnitude of the tail correction for each CRM on a turret-by-turret basis. Results from both tail correction methodologies are described below.

For major and minor isotope ratio measurements, the mass fractionation correction is performed as follows: Mass fractionation per amu is determined from the difference between the measured  $^{240}\text{Pu}/^{239}\text{Pu}$  major isotope ratio and the certified ratio decay corrected to the date of separation. This correction is performed on a per turret basis and the traceable isotopic standard used for estimation of the mass fractionation correction is known as the comparator standard. The mass fractionation estimate from the comparator is then applied to the other standards (QC standards) and the unknown samples (see [3, 5, or 8] for additional details). The per amu mass fractionation correction factor is then scaled and applied to the  $^{238}\text{Pu}/^{239}\text{Pu}$ ,  $^{241}\text{Pu}/^{239}\text{Pu}$ , and  $^{242}\text{Pu}/^{239}\text{Pu}$  minor isotope ratios. The tailing correction as described in the next section is applied to the minor isotope ratios that are already corrected for mass fractionation.

## Results and discussion

The tailing on the low mass side of a large beam is predominantly due to ions losing energy due to ion-neutral collisions. An increase in energy of the ions (to cause tailing on the high mass side) is not very likely. For this reason, the tailing on the low mass side is usually more pronounced. However, there can also be elastic scattering, or scattering with the effect of change

of the flight path of ions. This effect is probably a symmetric effect towards both sides of the large beam. Figure 1 shows the measured intensities at masses  $^{233}\text{U}$ ,  $^{234}\text{U}$ ,  $^{235}\text{U}$ ,  $^{236}\text{U}$ , and nominal mass 237 in a U sample with no significant signal at isotopes other than  $^{238}\text{U}$  [9, 10]. Figure 1 shows that the magnitude of the tail corrections decrease exponentially as mass difference with the  $^{238}\text{U}$  mass increases. At  $^{233}\text{U}$ , 5 amu below the  $^{238}\text{U}$  signal the ratio of the tail at  $^{233}\text{U}/^{238}\text{U}$  becomes similar to the noise levels achieved with the measurement system. Note that TIMS instrument manufacturers state the abundance sensitivity using U isotopes. The observed abundance sensitivity curve as shown in Fig. 1 is consistent with manufacturer specifications.

For performing tailing corrections at Pu, analytical laboratories use the abundance sensitivity curve such as that shown in Fig. 1 measured in a suitable uranium sample and assume that the magnitude of the tail correction stays similar on both low mass side and high mass side of the large beam. For the 6 V sum intensity used as target for TE analysis, the measured  $^{241}\text{Pu}$  and  $^{242}\text{Pu}$  signals are often large enough to make the tailing corrections (of similar magnitude as that shown in Fig. 1) an insignificant source of systematic bias in the  $^{241}\text{Pu}/^{239}\text{Pu}$  and  $^{242}\text{Pu}/^{239}\text{Pu}$  ratios. Table 2 shows the magnitude of the bias at all three minor isotope ratios  $^{238}\text{Pu}/^{239}\text{Pu}$ ,  $^{241}\text{Pu}/^{239}\text{Pu}$ , and  $^{242}\text{Pu}/^{239}\text{Pu}$ . Table 2 also shows that within the precision observed only the systematic bias at  $^{238}\text{Pu}/^{239}\text{Pu}$  isotope ratio is significant. For the  $^{241}\text{Pu}/^{239}\text{Pu}$  and  $^{242}\text{Pu}/^{239}\text{Pu}$  isotope ratios, within the precision, the bias overlap the “0” value indicating that the bias is not significant. Being only 1 amu below the  $^{239}\text{Pu}$ , dominant isotopic

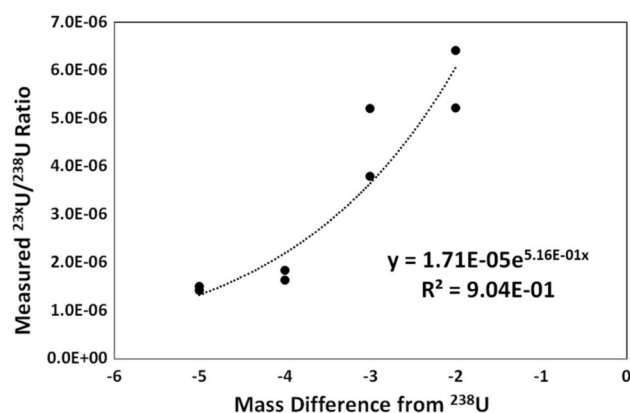


**Fig. 1** Tail contributions at masses < 238 amu, as measured in the natural uranium standard CRM 112-A [9]. This standard is free from  $^{233}\text{U}$  and  $^{236}\text{U}$  isotopes. Thus the tail contributions can be evaluated with a high degree of confidence at these isotopes

**Table 1** Cup configuration used for the TE analysis of Pu

Cup	L-2	L-1	Center	H-1	H-2	H-3
Isotope	$^{238}\text{Pu}$	$^{239}\text{Pu}$	$^{240}\text{Pu}$	$^{241}\text{Pu}$	$^{242}\text{Pu}$	$^{244}\text{Pu}$

**Table 2** Summary statistics observed on plutonium minor isotope ratio measurements

CRM	Isotope ratio	Average bias (%)	Std dev	Bias (per turret basis)	Std dev (bias per turret basis)
136	$^{238}\text{Pu}/^{239}\text{Pu}$	1.066	0.323	1.063	0.131
	$^{241}\text{Pu}/^{239}\text{Pu}$	0.317	0.297	0.361	0.068
	$^{242}\text{Pu}/^{239}\text{Pu}$	-0.034	0.133	-0.032	0.028
137	$^{238}\text{Pu}/^{239}\text{Pu}$	1.025	0.251	1.041	0.108
	$^{241}\text{Pu}/^{239}\text{Pu}$	0.301	0.188	0.287	0.030
	$^{242}\text{Pu}/^{239}\text{Pu}$	-0.153	0.054	-0.153	0.018
138	$^{238}\text{Pu}/^{239}\text{Pu}$	22.09	7.67	22.26	2.02
	$^{241}\text{Pu}/^{239}\text{Pu}$	0.098	0.348	0.130	0.098
	$^{242}\text{Pu}/^{239}\text{Pu}$	0.353	0.352	0.382	0.132
126-A	$^{238}\text{Pu}/^{239}\text{Pu}$	11.61	4.47	10.50	1.72
	$^{241}\text{Pu}/^{239}\text{Pu}$	0.000	0.205	-0.027	0.070
	$^{242}\text{Pu}/^{239}\text{Pu}$	0.169	0.406	0.207	0.170

signal in most plutonium materials, the tailing effect is the largest for the  $^{238}\text{Pu}/^{239}\text{Pu}$  isotope ratio.

The methodology for performing the systematic bias corrections using traceable CRMs is as follows: The deviations (expressed as a percent relative deviations, %RDs) of the measured minor isotope ratios from the certified values for these ratios are calculated. The average %RD observed for a specific ratio is then used to correct the unknown sample measured together with the standard aliquots measured as an auto sequence. Figure 1 shows that the even for measurements that are performed within a short duration, there is significant variability in the bias originating from the tailing. Often the standards are analyzed in triplicate (interspersed within the analysis sequence) within the same turret. Provided the measured minor isotope ratio of the sample is comparable to that of the CRM used for tailing correction, the systematic bias in the standard can be used to scale the unknown sample. The %RDs for each  $^{238}\text{Pu}/^{239}\text{Pu}$ ,  $^{241}\text{Pu}/^{239}\text{Pu}$ , and  $^{242}\text{Pu}/^{239}\text{Pu}$  minor isotope ratios are then control-charted to estimate the control limits ( $2\text{-}\sigma$  warning limits and  $3\text{-}\sigma$  alarm limits) for each isotope ratio and each isotopic standard.

Figure 2 shows the systematic biases in the  $^{238}\text{Pu}/^{239}\text{Pu}$  ratio. The %RDs for the  $^{238}\text{Pu}/^{239}\text{Pu}$  ratios in one high-burnup CRM and one low-burnup CRM (after correction using the two different tailing correction methodologies described above) are shown as examples. Data shown in the left panels have been corrected for systematic biases (using the abundance sensitivity curve shown in Fig. 1) and the right panels show data that have been corrected for systematic bias on a per-turret basis. Table 2 shows a summary of the analytical data from the present evaluation. Note

that for all four CRM standards, within the observed precision (%RSDs), systematic biases are significant only for the  $^{238}\text{Pu}/^{239}\text{Pu}$  ratio, as the %RDs (w.r.t the certified ratios decay corrected to the date of separation of the Pu isotopic fraction) overlap the “0.0” value for the  $^{241}\text{Pu}/^{239}\text{Pu}$  and  $^{242}\text{Pu}/^{239}\text{Pu}$  ratios (with the exception of the  $^{242}\text{Pu}/^{239}\text{Pu}$  ratio in CRM 137, which is discussed below). This is consistent with expectations as the isotopic abundance of this isotope is the smallest in most nuclear material samples (for low burn-up and high burn-up materials) and the magnitude of the tailing correction is the largest for this ratio as the  $^{238}\text{Pu}$  isotope is only 1 amu lower than the most abundant isotope,  $^{239}\text{Pu}$ . Small negative biases in the  $^{242}\text{Pu}/^{239}\text{Pu}$  minor ratio observed for CRM 137 might be indicating an offset between true value and the certified value for this minor isotope ratio. For the  $^{238}\text{Pu}/^{239}\text{Pu}$  ratio in CRM 136, an average bias of 1.07% is observed. The data yield a  $2\text{-}\sigma$  warning limit of 0.65%. The abundance sensitivity correction, if truly representing the tail correction at  $^{238}\text{Pu}$  would shift the average bias in the  $^{238}\text{Pu}/^{239}\text{Pu}$  to the zero line, with the scatter of the %RD values staying the same. The average bias observed in the  $^{238}\text{Pu}/^{239}\text{Pu}$  ratio, when the systematic biases are corrected on a per turret basis, is 1.06%. When the tailing corrections are performed on a per turret basis, the  $2\text{-}\sigma$  warning limit, however, improves to 0.31%. For the  $^{238}\text{Pu}/^{239}\text{Pu}$  ratio in CRM 126-A, an average bias of 11.86% is observed (compared to average bias of 10.50% for tailing corrections on a per turret basis). The  $2\text{-}\sigma$  warning limits for the  $^{238}\text{Pu}/^{239}\text{Pu}$  ratio data using the abundance sensitivity correction factor and per turret tailing correction are 9.5% and 3.3%, respectively. Note also that tailing corrections based on the abundance sensitivity corrections such as that

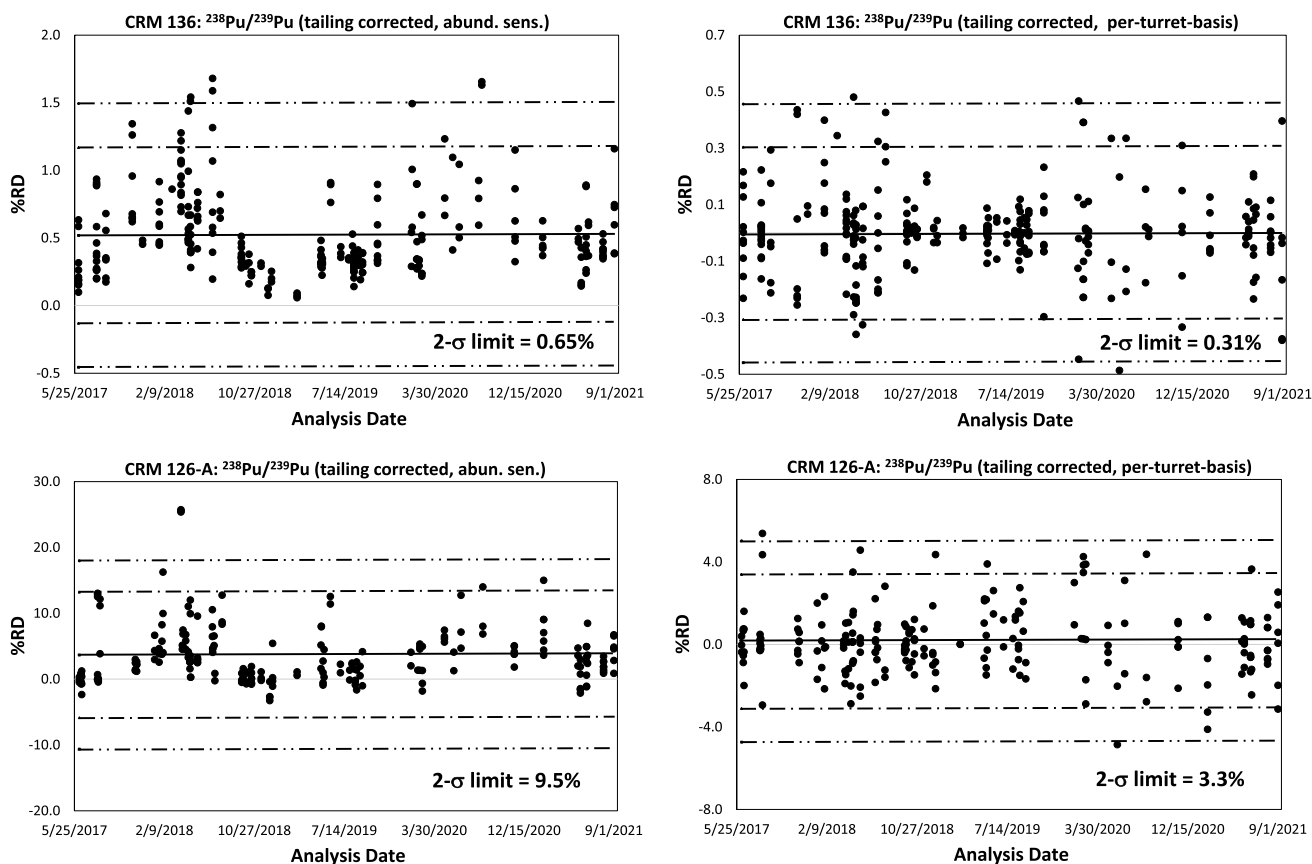


**Fig. 2** Percent relative deviations (%RDs) of the  $^{238}\text{Pu}/^{239}\text{Pu}$  ratios in CRMs 136 (top panels) and 126-A (bottom panels) from the certified values for these CRMs. The left panel shows data corrected for tailing

corrections based on abundance sensitivity (as shown in Fig. 1) and right panel shows data that are corrected for bias on a per turret basis

obtained from the tail measurements on a depleted or natural U standard often yields a residual bias in the  $^{238}\text{Pu}/^{239}\text{Pu}$  and other minor ratios of Pu (see Table 3 data for additional details).

Table 3 shows the measured signal intensities (in mV units) at the different isotopes  $^{238}\text{Pu}$ ,  $^{239}\text{Pu}$ ,  $^{240}\text{Pu}$ ,  $^{241}\text{Pu}$ , and  $^{242}\text{Pu}$  for all four CRM standards (CRMs 136, 137, 138, and 126-A) included in this investigation. The corrections for tailing (also in mV units) based on the abundance sensitivity as well as that estimated from the systematic bias observed on a per-turret basis are also listed.

Figure 3 shows the systematic bias in the  $^{241}\text{Pu}/^{239}\text{Pu}$  ratio for a high-burnup (CRM 137) and a low-burnup (CRM 126-A) standard. For both CRMs, the left panel shows the measured systematic biases in the  $^{241}\text{Pu}/^{239}\text{Pu}$  minor isotope ratio and the right panel shows control charts when the

bias correction is performed on a per turret basis. The  $2-\sigma$  warning limits obtained using the two different approaches to tailing corrections are 0.38% and 0.08% (for CRM 137) and 0.44% and 0.26% (for CRM 126-A). For this isotope ratio, data marked by the ellipsoidal represent an additional column wash to remove the  $^{241}\text{Am}$  from the analyzed Pu isotopic fraction. Figure 3 shows that the additional column wash improved the precision of the  $^{241}\text{Pu}/^{239}\text{Pu}$  ratio, indicating complete removal of the  $^{241}\text{Am}$  from the Pu fraction ( $^{241}\text{Am}$  is an isobaric interference at  $^{241}\text{Pu}$ ). With two columns washes that was used to remove  $^{241}\text{Am}$  from the Pu isotopic fraction, a small amount of  $^{241}\text{Am}$  was left in the Pu isotopic fraction that was measured.

Figure 4 shows the systematic bias in the  $^{242}\text{Pu}/^{239}\text{Pu}$  ratio for a high-burnup (CRM 137) and a low-burnup (CRM 138) standard. For both CRMs, the left panel shows the measured

**Table 3** Signal Intensities (in mV units) measured at different Pu isotopes for a TE analysis using a 6 V target intensity and expected based on the observed bias in the isotope ratio

CRM	Isotope	Signal intensity (mV)		Tail correction (mV)		
		Measured	Bias corrected <sup>#</sup>	Abundance sensitivity*	Per turret bias <sup>§</sup>	Residual bias <sup>**</sup>
136	<sup>238</sup> Pu	12.419	12.277	0.067	0.142	0.075
	<sup>239</sup> Pu	5049.90	5049.90	None	None	None
	<sup>240</sup> Pu	867.88	867.910	0.062	−0.027	−0.089
	<sup>241</sup> Pu	28.999	28.902	0.046	0.097	0.051
	<sup>242</sup> Pu	40.799	40.816	0.022	−0.016	−0.039
137	<sup>238</sup> Pu	16.279	16.098	0.070	0.181	0.111
	<sup>239</sup> Pu	4409.95	4409.95	None	None	None
	<sup>240</sup> Pu	1444.35	1444.28	0.062	0.070	0.008
	<sup>241</sup> Pu	35.929	35.806	0.052	0.123	0.071
	<sup>242</sup> Pu	93.497	93.649	0.023	−0.152	−0.175
138	<sup>238</sup> Pu	0.5997	0.4883	0.0644	0.1114	0.0471
	<sup>239</sup> Pu	5477.00	5477.00	None	None	None
	<sup>240</sup> Pu	516.96	516.66	0.06	0.30	0.24
	<sup>241</sup> Pu	3.2652	3.2565	0.0418	0.0087	−0.0331
	<sup>242</sup> Pu	2.1685	2.1605	0.0219	0.0080	−0.0139
126-A	<sup>238</sup> Pu	0.7746	0.6896	0.0635	0.0850	0.0215
	<sup>239</sup> Pu	5616.39	5616.39	None	None	None
	<sup>240</sup> Pu	376.12	376.00	0.061	0.11	0.052
	<sup>241</sup> Pu	4.4065	4.4067	0.0404	−0.0002	−0.041
	<sup>242</sup> Pu	2.3117	2.3089	0.0219	0.0029	−0.019

Note that correcting for tailing effects based on abundance sensitivity leaves “residual bias” in the isotope abundance (the magnitude of the “residual bias” is dependent on the isotopic make-up of the standard).

\* the magnitude of the tail correction predicted from the abundance sensitivity curve shown in Fig. 1 and the <sup>239</sup>Pu and <sup>240</sup>Pu signals measured are shown in mV units.

# the bias corrected isotopic signals in mV units (with bias corrections performed on a per turret basis) are shown.

§ the magnitude of the bias correction (on a per turret basis) are shown in mV units.

\*\* residual bias is the bias that would have been remaining in the isotopic abundance measurements, if the bias correction was performed based on manufacturers stated abundance sensitivity or abundance sensitivity actually measured as in Fig. 1

systematic biases in the <sup>242</sup>Pu/<sup>239</sup>Pu minor isotope ratio and the right panel shows control charts when the bias correction is performed on a per turret basis. The 2-σ warning limits obtained using the two different approaches to tailing corrections are 0.12% and 0.04% (for CRM 137) and 0.70% and 0.30% (for CRM 138).

### Uncertainty budgets for plutonium minor isotope ratios

Uncertainty budgets for the minor isotope ratios were calculated following GUM methodologies [14–16]. The model equations used for the uncertainty calculations are as follows:

$$\left(\frac{{}^{238}\text{Pu}}{{}^{239}\text{Pu}}\right)_{\text{corrected}} = \left(\frac{{}^{238}\text{Pu}}{{}^{239}\text{Pu}}\right)_{\text{measured}} * \delta_{238\text{tail}} * \delta_{\text{fractionation}} \quad (1)$$

$$\left(\frac{{}^{241}\text{Pu}}{{}^{239}\text{Pu}}\right)_{\text{corrected}} = \left(\frac{{}^{241}\text{Pu}}{{}^{239}\text{Pu}}\right)_{\text{measured}} * \delta_{241\text{tail}} * \delta_{\text{fractionation}} \quad (2)$$

$$\left(\frac{{}^{242}\text{Pu}}{{}^{239}\text{Pu}}\right)_{\text{corrected}} = \left(\frac{{}^{242}\text{Pu}}{{}^{239}\text{Pu}}\right)_{\text{measured}} * \delta_{242\text{tail}} * \delta_{\text{fractionation}} \quad (3)$$

In addition to the measured variability in the minor isotope ratio of the specific CRM ( $\left(\frac{{}^{238}\text{Pu}}{{}^{239}\text{Pu}}\right)_{\text{measured}}$ ,  $\left(\frac{{}^{241}\text{Pu}}{{}^{239}\text{Pu}}\right)_{\text{measured}}$ , and  $\left(\frac{{}^{242}\text{Pu}}{{}^{239}\text{Pu}}\right)_{\text{measured}}$ ), uncertainty factors also arise from tailing correction as observed variability in the tailing correction for the specific ratio ( $\delta_{238\text{tail}}$ ,

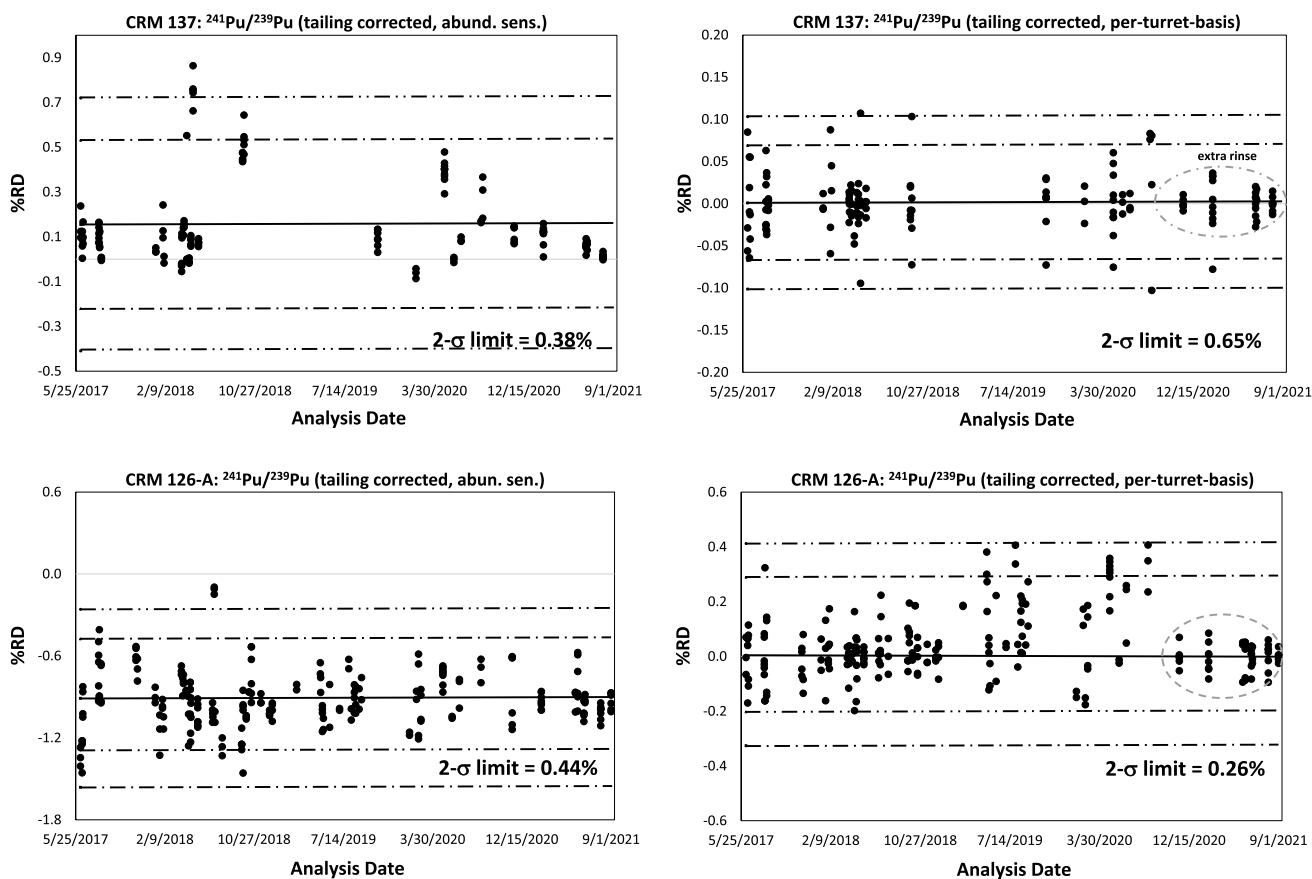


**Fig. 3** Percent relative deviations (%RDs) of the  $^{241}\text{Pu}/^{239}\text{Pu}$  ratios in CRMs 136 (top panels) and 126-A (bottom panels) from the certified values for these CRMs. The left panel shows data corrected for tailing based on abundance sensitivity (as shown in Fig. 1) and right panel

shows data that are corrected for bias on a per turret basis. Measurements indicated in the ellipsoidal received an additional rinse with 12 M HCl to remove the  $^{241}\text{Am}$ , which is an isobaric interference at  $^{241}\text{Pu}$

$\delta_{241\text{tail}}$ , and  $\delta_{242\text{tail}}$ ), and uncertainty in the fractionation correction factor, as determined from the variability in the mass fractionation correction factor ( $\delta_{\text{fractionation}}$ ). Mass fractionation is determined by comparing the measured  $^{240}\text{Pu}/^{239}\text{Pu}$  major isotope ratio with the certified value decay corrected to the date of separation of the Pu isotopic fraction. The difference is then scaled to the other isotope ratios using the mass difference from  $^{239}\text{Pu}$  on a per turret basis using the comparator CRM.

Table 3 shows the measured signals at the different Pu isotopes and the magnitude of the tail corrections. Table 2 data showed that the systematic bias obtained for each

isotope ratio using the two different methodologies for tailing correction (correction based on abundance sensitivity and on per-turret-basis correction) were similar. However, Table 3 data shows that the systematic biases at the minor isotope ratios are not fully accounted for when the tailing corrections are made used using an assumed abundance sensitivity correction factor. Table 3 also shows that the magnitude of the “residual bias” (difference between the actual bias and the bias expected based on abundance sensitivity correction) can be as large or larger than the correction due to the abundance sensitivity.



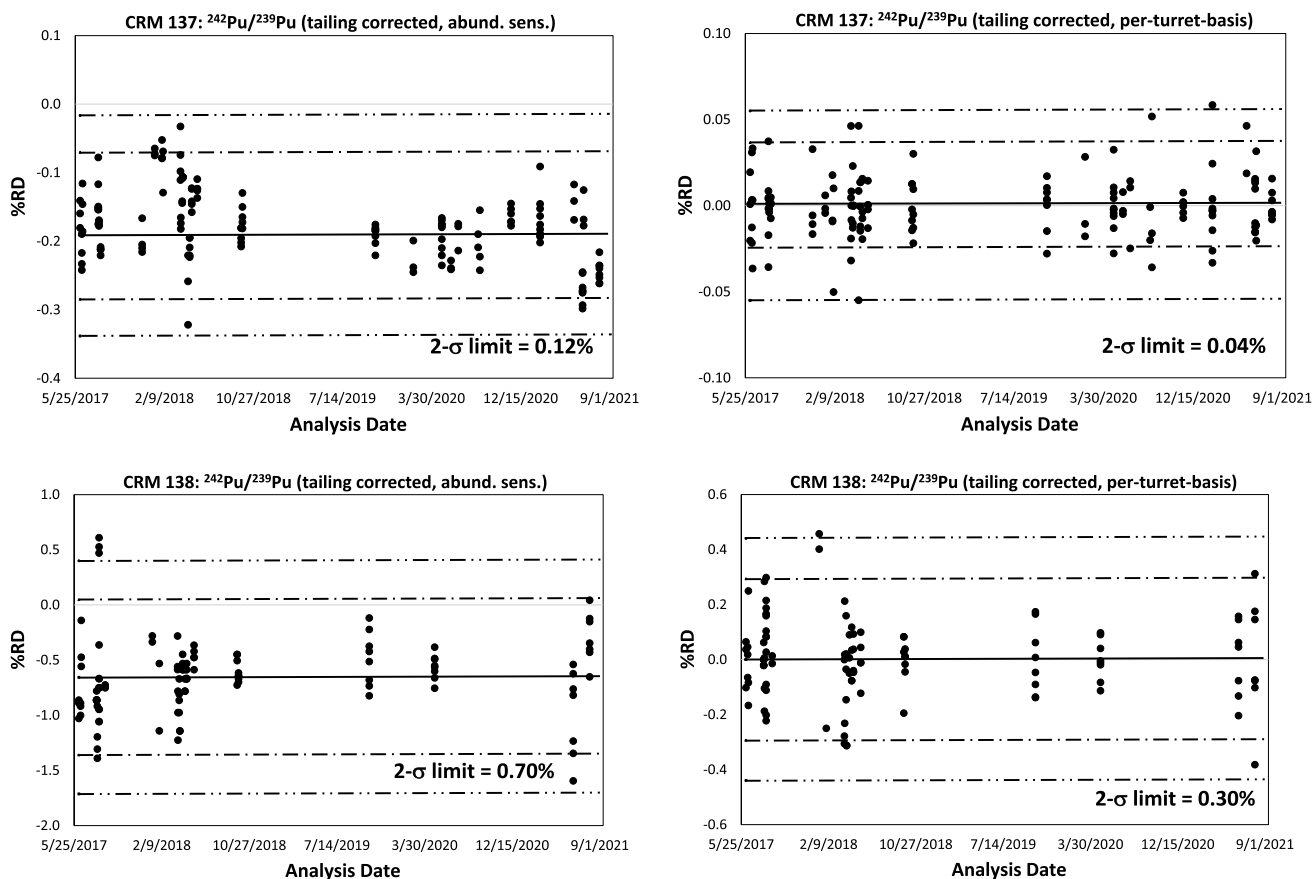


**Fig. 4** Percent relative deviations (%RDs) of the  $^{242}\text{Pu}/^{239}\text{Pu}$  ratios in CRMs 136 (top panels) and 138 (bottom panels) from the certified values for these CRMs. The left panel shows all data and right panel shows data that are corrected for bias on a per turret basis

A summary of the uncertainty budgets for the  $^{238}\text{Pu}/^{239}\text{Pu}$ ,  $^{241}\text{Pu}/^{239}\text{Pu}$ , and  $^{242}\text{Pu}/^{239}\text{Pu}$  minor isotope ratios are provided in the two high-burnup standards (Table 4, CRMs 136 and 137) and the two low-burnup standards (Table 5, CRMs 138 and 126-A). Uncertainty in the tailing correction dominates the uncertainty budget for all these Pu isotope ratios. Precision of the minor isotope ratio measurements makes contributions in some instances, especially for the  $^{238}\text{Pu}/^{239}\text{Pu}$  isotope ratio. Uncertainty parameters like the variability in the mass fractionation correction factor makes no contributions to the uncertainty budgets of the  $^{238}\text{Pu}/^{239}\text{Pu}$ ,  $^{241}\text{Pu}/^{239}\text{Pu}$ , and  $^{242}\text{Pu}/^{239}\text{Pu}$  minor isotope ratios.

## Conclusions

We investigated the uncertainty in the minor Pu isotope ratios for two different approaches at performing the tailing correction. The first approach using the manufacturer specified abundance sensitivity correction factors yielded uncertainties larger than those obtained using corrections for tailing on a per turret basis. The uncertainty factors for the minor isotope ratios using these different approaches are described in the paper. The latter approach yielded minor isotope data with no “residual bias” and lower uncertainty limits and is the superior methodology for correcting the systematic biases.

**Table 4** Uncertainty budgets for minor isotope ratios of high-burnup Pu standards

CRM	Isotope ratio	Tailing correction	Nominal value	Relative uncertainty (%)	Uncertainty contribution
136	$^{238}\text{Pu}/^{239}\text{Pu}$	Abundance sensitivity factor	0.002046	0.65	Abundance sensitivity (99.4%), precision of the $^{238}\text{Pu}/^{239}\text{Pu}$ ratio (0.6%)
		bias corrected on a per turret basis	0.0020462	0.31	Bias correction from tailing (97.4%), precision of the $^{238}\text{Pu}/^{239}\text{Pu}$ ratio (2.6%)
	$^{241}\text{Pu}/^{239}\text{Pu}$	Abundance sensitivity factor	0.004817	0.59	Abundance sensitivity (99.7%), precision of the $^{238}\text{Pu}/^{239}\text{Pu}$ ratio (0.3%)
		bias corrected on a per turret basis	0.004817	0.24	Bias correction from tailing (98.4%), precision of the $^{238}\text{Pu}/^{239}\text{Pu}$ ratio (1.6%)
	$^{242}\text{Pu}/^{239}\text{Pu}$	Abundance sensitivity factor	0.006803	0.27	Abundance sensitivity (98.7%), precision of the $^{238}\text{Pu}/^{239}\text{Pu}$ ratio (1.3%)
		bias corrected on a per turret basis	0.0068026	0.086	Bias correction from tailing (87.4%), precision of the $^{238}\text{Pu}/^{239}\text{Pu}$ ratio (12.3%)
137	$^{238}\text{Pu}/^{239}\text{Pu}$	Abundance sensitivity factor	0.002683	0.50	Abundance sensitivity (99%), precision of the $^{238}\text{Pu}/^{239}\text{Pu}$ ratio (1%)
		bias corrected on a per turret basis	0.0026830	0.25	Bias correction from tailing (95.8%), precision of the $^{238}\text{Pu}/^{239}\text{Pu}$ ratio (4.2%)
	$^{241}\text{Pu}/^{239}\text{Pu}$	Abundance sensitivity factor	0.005968	0.38	Abundance sensitivity (99.4%), precision of the $^{238}\text{Pu}/^{239}\text{Pu}$ ratio (0.6%)
		bias corrected on a per turret basis	0.0059677	0.078	Bias correction from tailing (84.9%), precision of the $^{238}\text{Pu}/^{239}\text{Pu}$ ratio (14.7%)
	$^{242}\text{Pu}/^{239}\text{Pu}$	Abundance sensitivity factor	0.015608	0.11	Abundance sensitivity (92.7%), precision of the $^{238}\text{Pu}/^{239}\text{Pu}$ ratio (7.1%)
		bias corrected on a per turret basis	0.0156081	0.064	Bias correction from tailing (77.2%), precision of the $^{238}\text{Pu}/^{239}\text{Pu}$ ratio (22.2%)

**Table 5** Uncertainty budgets for minor isotope ratios of low-burnup plutonium standards

CRM	Isotope ratio	Tailing correction	Nominal value	Relative uncertainty (%)	Uncertainty contribution
138	$^{238}\text{Pu}/^{239}\text{Pu}$	Abundance sensitivity factor	0.000081	15	Abundance sensitivity (100%)
		bias corrected on a per turret basis	0.0000814	3.9	Variability of the bias from tailing (100%)
	$^{241}\text{Pu}/^{239}\text{Pu}$	Abundance sensitivity factor	0.0005427	0.70	Abundance sensitivity (99.3%), precision of the $^{238}\text{Pu}/^{239}\text{Pu}$ ratio (0.7%)
		bias corrected on a per turret basis	0.0005427	0.26	Variability of the bias from tailing (94.8%), precision of the $^{238}\text{Pu}/^{239}\text{Pu}$ ratio (5.2%)
	$^{242}\text{Pu}/^{239}\text{Pu}$	Abundance sensitivity factor	0.0003601	0.70	Abundance sensitivity (99.3%), precision of the $^{238}\text{Pu}/^{239}\text{Pu}$ ratio (0.7%)
		bias corrected on a per turret basis	0.0003601	0.31	Variability of the bias from tailing (96.1%), precision of the $^{238}\text{Pu}/^{239}\text{Pu}$ ratio (3.8%)
126-A	$^{238}\text{Pu}/^{239}\text{Pu}$	Abundance sensitivity factor	0.000115	9.3	Abundance sensitivity (100%)
		bias corrected on a per turret basis	0.0001150	3.6	Variability of the bias from tailing (100%)
	$^{241}\text{Pu}/^{239}\text{Pu}$	Abundance sensitivity factor	0.0007363	0.50	Abundance sensitivity (98.5%), precision of the $^{238}\text{Pu}/^{239}\text{Pu}$ ratio (1.5%)
		bias corrected on a per turret basis	0.0007363	0.37	Variability of the bias from tailing (97.3%), precision of the $^{238}\text{Pu}/^{239}\text{Pu}$ ratio (2.6%)
	$^{242}\text{Pu}/^{239}\text{Pu}$	Abundance sensitivity factor	0.0003848	0.87	Abundance sensitivity (99.5%), precision of the $^{238}\text{Pu}/^{239}\text{Pu}$ ratio (0.5%)
		bias corrected on a per turret basis	0.0003848	0.55	Variability of the bias from tailing (98.8%), precision of the $^{238}\text{Pu}/^{239}\text{Pu}$ ratio (1.2%)



**Acknowledgements** Discussions with colleagues S. Floyd (LLNL), L. Tandon (LANL), A. Olson (LANL), S. Richter (IRMM), and P. Mason (NBL-PO) on TIMS isotopic data uncertainties are gratefully acknowledged. Authors have no conflict of interest to declare. All authors have reviewed the paper and approved the content. Authors are grateful to an anonymous reviewer for a very detailed review and comments. Revisions performed as a result of these comments have improved the quality of the paper.

## References

1. Romkowski M, Franzini S, Koch L (1987) Mass-spectrometric analysis of sub-nanocurie samples of uranium and plutonium. In: Proceedings of the 8th annual ESARDA symposium, London, 12–14
2. Richter S, Goldberg SA (2003) Improved techniques for high accuracy isotope ratio measurements of nuclear materials using thermal ionization mass spectrometry. *Int J Mass Spectrom* 229:181–197
3. Mathew KJ, O'Connor G, Hasozbek A, Kraiem MJ (2013) Total evaporation method for uranium isotope-amount ratio measurements. *J Anal At Spectrom* 28:866–876
4. Callis EL, Abernathy RM (1991) High-precision isotopic analyses of uranium and plutonium by total sample volatilization and signal integration. *Int J Mass Spectrom* 103:93–105
5. Mathew KJ, Ottenfeld CF, Keller RC, Kuhn KJ, Fulwyler JB (2020) Preparation of  $^{241}\text{Am}/^{243}\text{Am}$  gravimetric mixtures and development of Am isotopic and assay measurement techniques using thermal ionization mass spectrometry. *Int J Mass Spectrom* 458:116430
6. Richter S, Kühn K, Aregbe Y, Hedberg M, Horta-Domenech J, Mayer K, Zuleger E, Bürger S, Boulyga S, Köpf A, Poths J, Mathew K (2011) Improvements in routine uranium isotope ratio measurements using the modified total evaporation method for multi-collector thermal ionization mass spectrometry. *J Anal At Spectrom* 26:550–564
7. Mathew KJ, Canaan RD, Hexel C, Giaquinto J, Krichinsky AM (2015) Qualification and initial characterization of a high-purity  $^{233}\text{U}$  spike for use in uranium analyses. *Int J Mass Spectrom* 389:47–53
8. Mathew KJ, Essex RM, Hasozbek A, Orłowicz G, Soriano M (2014) Uranium isotope-amount ratios in certified reference material 116-A – uranium (enriched) metal assay and isotopic standard. *Int J Mass Spectrom* 369:48–58
9. Mathew KJ, Mason P, Voeks A, Narayanan U (2012) Uranium isotope abundance ratios in natural uranium metal certified reference material 112-A. *Int J Mass Spectrom* 315:8–14
10. Mathew KJ, Singleton GL, Essex RM, Hasozbek A, Orłowicz G, Soriano M (2013) Characterization of the uranium isotopic abundances in depleted uranium metal assay standard. *J Radioanal Nucl Chem* 296:435–440
11. Mialle S, Quémet A, Ponvienne A, Gourgiotis A, Aubert M, Isnard H, Chartier F (2012) The use of total evaporation method using channeltron electron multipliers by thermal ionization mass spectrometry for europium isotope ratio measurements on pictogram sample amounts. *Int J Mass Spectrom* 309:141–147
12. Richter S, Alonso A, Aregbe Y, Eykens R, Kehoe F, Kühn H, Kivel N, Verbruggen A, Wellum R, Taylor PDP (2009) A new series of uranium isotope reference materials for investigating linearity of secondary electron multipliers in isotope mass spectrometry. *Int J Mass Spectrom* 281:115–125
13. Mialle S, Richter S, Hennessy C, Truyens J, Jacobsson U, Aregbe Y (2015) Certification of uranium hexafluoride reference materials for isotopic composition. *J Radioanal Nucl Chem* 305:255–266
14. Burger S, Essex RM, Mathew KJ, Richter S, Thomas RB (2010) Implementation of guide to the expression of uncertainty in measurement (GUM) to multi-collector TIMS uranium isotope ratio metrology. *Int J Mass Spectrom* 294:65–76
15. BIPM JCGM 100 (2008) (GUM 1995 with minor corrections), evaluation of measurement data – guide to the expression of uncertainty in measurement. bureau international des poids et mesures, sevres cedex, France ([www.bipm.org](http://www.bipm.org))
16. QUAM (2012) Quantifying uncertainty in analytical measurement – eurachem, 3rd edn, EURACHEM/CITAG Guide CG4

**Publisher's Note** Springer Nature remains neutral with regard to jurisdictional claims in published maps and institutional affiliations.

Springer Nature or its licensor holds exclusive rights to this article under a publishing agreement with the author(s) or other rightsholder(s); author self-archiving of the accepted manuscript version of this article is solely governed by the terms of such publishing agreement and applicable law.